Surface Science 606 (2012) 858–864

Contents lists available at SciVerse ScienceDirect

Surface Science

journal homepage: www.elsevier.com/locate/susc

The interaction of H_2O molecules with iron films studied with MIES, UPS and XPS

K. Volgmann [a,c], F. Voigts [a], W. Maus-Friedrichs [a,b,*]

[a] Institut für Physik und Physikalische Technologien, Technische Universität Clausthal, Leibnizstrasse 4, 38678 Clausthal-Zellerfeld, Germany
[b] Clausthaler Zentrum für Materialtechnik, Leibnizstrasse 4, 38678 Clausthal-Zellerfeld, Germany
[c] Institut für Physikalische Chemie und Elektrochemie, Gottfried Wilhelm Leibniz Universität Hannover, Callinstr. 3 – 3a, 30167 Hannover, Germany

ARTICLE INFO

Article history:
Received 7 July 2011
Accepted 1 February 2012
Available online 10 February 2012

Keywords:
Metastable induced electron spectroscopy
Ultraviolet photoelectron spectroscopy
X-ray photoelectron spectroscopy
Iron
Iron oxide
H_2O

ABSTRACT

X-Ray Photoelectron Spectroscopy (XPS), Metastable Induced Electron Spectroscopy (MIES) and Ultraviolet Photoelectron Spectroscopy (UPS) were applied to study the interaction of H_2O molecules with iron films. During the interaction with H_2O molecules under ultrahigh vacuum conditions, an oxide film is formed on the iron surface. UPS and XPS still show metallic contributions, even for a surface which is exposed to about 10^3 L. The oxide film thickness amounts to about 1.8 nm. No hydroxide formation is observed at all, neither in UPS nor in MIES. Further impinging H_2O molecules do not interact with the surface, because the oxide film inhibits the dissociation of impinging molecules.
H_2O exposure beyond 10^9 L does not lead to a significant increase of the oxide layer, which saturates at a thickness of 1.8 nm. In particular, no surface hydroxide is observed at this exposure. Neither XPS UPS nor MIES reveal any indication for this.

1. Introduction

Iron is known to be very corroding under ambient conditions. Complex electrochemical models have been employed to explain the corrosion and the corrosion pathways (see for example [1,2]). Iron is reported to be very reactive against SO_2, HCl and moderate reactive against O_2, H_2O, CO_2 and organic acids like HCOOH. Following the macroscopic picture the formation of rust layers is a three step process [1]:

1. Formation of a thin oxide/hydroxide layer with a thickness between 1 nm and 4 nm within several milliseconds. This film is found to be stable and passivating in the absence of atmospheric impurities as well as in the absence of relative humidities beyond 60%.
2. In aqueous environments (humidities beyond 60%) this oxide/hydroxide layer changes into one of two types of green rust ($Fe_2O_x(OH)_y$) or ($Fe_3O_x(OH)_y$), which both consists of Fe^{2+} und Fe^{3+} within several hours.
3. Transformation into the fragile brown rust consisting of iron oxides and hydroxides (Fe^{3+} only) subsequently.

Following literature these macroscopically described processes only require an aqueous atmosphere with a humidity of at least 60%.

Another couple of recent publications deal with the reaction of water with iron [3–6]. A common observation is the growth of a passivating oxide layer. The adsorption of large amounts of OH groups is only detected at high water exposures ($>10^4$ L) [3]. The proposed model of Grosvenor et al. for the rate-limiting step is the generation of hydrogen atoms because of the H_2O dissociation at the surface. These can either hinder the diffusion in the oxide layer or block vacant surface sites and thus hinder a further dissociation [3]. Another suggestion by [4] is the formation of Fe^{3+} cations which might also have an influence on the adsorption onto and on the diffusion into the surface layer. The adsorbed OH groups are not incorporated into the lattice but chemisorbed on top of the iron oxide layer which is shown by Angular-Resolved Photoelectron Spectroscopy (ARPES) measurements [3].

A publication by Roberts and Wood deals with the investigation of the interaction of water vapor with iron surfaces applying X-ray Photoelectron Spectroscopy (XPS) [7]. They expose iron surfaces to a variable water partial pressure of 10^{-7} to 10^{-1} torr. Their work supports the macroscopic view, e. g. proposing a passivating iron oxide layer with a maximum thickness of 20 Å. We will show in this publication that we can confirm these results, but we can moreover provide additional information on the processes happening on the topmost surface layer of an iron film applying Metastable Induced Electron Spectroscopy (MIES).

This method has been applied before for the interaction of oxygen molecules with the iron surface by our group [8]. We found that even an oxygen saturated surface shows a metallic Fe contribution in XPS. The dissociation of oxygen molecules is hindered as soon as a certain coverage with iron oxide is achieved. Another result is that the

* Corresponding author at: Institut für Physik und Physikalische Technologien, Technische Universität Clausthal, Leibnizstrasse 4, 38678 Clausthal-Zellerfeld, Germany. Tel.: +49 5323 722310; fax: +49 5323 723600.
E-mail address: w.maus-friedrichs@pe.tu-clausthal.de (W. Maus-Friedrichs).

0039-6028/$ – see front matter © 2012 Elsevier B.V. All rights reserved.
doi:10.1016/j.susc.2012.02.002

interaction of He* atoms with the iron oxide surface during MIES takes place via the Auger Neutralization (AN) process. This result is surprising due to the fact that metal oxides usually show an Auger deexcitation (AD) process in MIES. In this case this is not observed due to the high work function of the iron oxide surface and the fact that intrinsic defects result in a Fermi level pinning to the conduction band.

Some publications already investigated the interaction of water with iron films by means of MIES [9–12]. We found that [11] discusses the interaction of H_2O with the system Na/Fe(001). All these references focus on the spin polarization or magnetic properties of the surface. Our focus on the passivating behavior and the formation of an oxide/hydroxide layer on the iron film is not investigated yet.

Thus, another aspect of this publication besides the aspect of corrosion is the investigation of iron surfaces exposed to high water partial pressures by means of MIES. In more detail the interaction path of the He* in front of the H_2O saturated iron surface will be revealed.

The overall scope of this paper is therefore the analysis of the surface reactions between iron films and water molecules under controlled vacuum conditions. XPS, Ultraviolet Photoelectron Spectroscopy (UPS) and MIES are applied to investigate the processes taking place at the topmost surface layer.

2. Experimental

An ultra high vacuum apparatus with a base pressure of $5 \cdot 10^{-11}$ mbar is used to carry out the experiments. All measurements were performed at room temperature.

Electron spectroscopy is performed using a hemispherical analyzer (VSW HA100) in combination with a source for metastable helium atoms (mainly He* $^3S_1$) and ultraviolet photons (He I line). A non-monochromatic X-ray source (Specs RQ20/38C) is utilized for XPS.

X-ray photons hit the surface under an angle of 80° to the surface normal, illuminating a spot of several mm in diameter. The Al K_α line with a photon energy of 1486.6 eV is used for all measurements presented here. Electrons are detected by the hemispherical analyzer with an energy resolution of 1.1 eV under an angle of 10° to the surface normal. All XPS spectra are displayed as a function of binding energy with respect to the Fermi level.

For quantitative XPS analysis, the photoelectron peak areas are calculated after background correction. Especially the strong increase of the inelastic background at the Fe 2p signal has to be corrected with either the method of Tougaard [13] or Shirley [14]. We use the Shirley method as we achieve the most consistent results for our measurements. This was also applied successfully for the interaction of iron with oxygen molecules [8]. Peak fitting with Gauss-type profiles was performed using OriginPro 7 G including the PFM fitting module which uses the Levenberg–Marquardt algorithms to achieve the best agreement possible between experimental data and fit. The quality of the fit is expressed by χ^2 which is returned by the PFM fitting module.

$$\chi^2(P) = \frac{S(P)}{d} = \frac{S(P)}{n^{eff} - p} \quad (1)$$

$S(P)$ denotes the sum of squares of the difference between the data and the fit with P being the parameter vector. The parameter vector P consists of FWHM, peak center and peak area for every used peak. The Levenberg-Marquardt algorithm minimizes $S(P)$ finding the best parameter vector P. Furthermore, d denotes the degree of freedom, n^{eff} is the number of data points used in the fit and p is the number of varying parameters in fitting. For best fit results, we always run the fitting procedure until the fit converges and returns a minimal χ^2 value. To optimize our fitting procedure, Voigt-profiles have been applied to various oxidic and metallic systems but for most systems the Lorentzian contribution converges to 0. Therefore all XPS peaks are fitted with Gaussian shapes. Nevertheless, all results are checked whether they are reasonable and consistent compared to the results by MIES and UPS. We also regard the discussion in literature dealing with this particular topic for iron and its oxides [15,16]. Therefore, we will not deal with any quantitative XPS analysis in this paper.

Photoelectric cross sections as calculated by Scofield [17] and inelastic mean free paths from the NIST database [18] as well as the transmission function of our hemispherical analyzer are taken into account when calculating stoichiometry. Essentially, the peak fitting procedure is done as described in [8].

MIES and UPS are performed applying a cold cathode gas discharge via a two-stage pumping system. A time-of-flight technique is employed to separate He* atoms (for MIES) from HeI photons (for UPS). Electrons emitted by He* interaction with the surface and photoelectrons are detected alternately at a frequency of 2000 Hz. Thus, both spectra are recorded quasi-simultaneously. The recording of such a MIES/UPS spectrum requires 280 s. The combined He*/He I beam strikes the sample surface under an angle of 45° to the surface normal and illuminates a spot of approximately 2 mm in diameter. The spectra are recorded by the hemispherical analyzer with an energy resolution of 220 meV under normal emission.

MIES is an extremely surface sensitive technique probing solely the outermost layer of the sample, because the He* atoms interact with the surface typically 0.3 to 0.5 nm in front of it. This may occur via a number of different mechanisms depending on surface electronic structure and work function, as described in detail elsewhere [19–21]. Only the processes relevant for the spectra presented here shall be discussed shortly:

During AD, an electron from the sample fills the 1s orbital of the impinging He*. Simultaneously, the He 2s electron carrying the excess energy is emitted. The resulting spectra reflect the Surface Density of States (SDOS) directly. AD-MIES and UPS can be compared and allow a distinction between surface and bulk effects. AD takes place for oxide surfaces and metal or semiconductor surfaces with work functions below about 3.5 eV.

The AN process occurs at pure and partly oxidized metal or semiconductor surfaces with work functions beyond 3.5 eV [22,23]. The impinging He* atom is ionized by a resonant transfer (RT) of its 2s electron into unoccupied surface states beyond the Fermi level. Afterwards, the remaining He^+ ion is neutralized by a surface electron thus emitting a second surface electron carrying the excess energy. The observed electron spectrum is rather structureless and represents a self convolution of the SDOS.

All MIES and UPS data have been corrected for the analyzer transmission function, that is proportional to E^{-1} in this energy range, where E denotes the kinetic energy of the electrons. The spectra are displayed as a function of the electron binding energy with respect to the Fermi level. The surface work function can be determined from the high binding energy onset of the MIES or the UPS spectra with an accuracy of ± 0.1 eV.

Iron films were prepared by evaporating iron (Goodfellow, 99.95% pure) with a commercial UHV evaporator (Omicron EFM3) onto a tungsten foil with 0.2 mm thickness (PLANSEE Composite Materials GmbH, 99.97% pure). It has been shown previously [8] that W is well suited as substrate, its interaction with iron atoms is negligible. These W foils are polycrystalline. For the growth of iron on W(110) [24] no crystalline growth is expected because of the large misfit of 9.4%. The W target is cleaned from surface contaminations by heating to approximately 1425 K prior to deposition. Iron is subsequently offered at a rate of 0.35 nm/min for 45 min at room temperature. This procedure results in an iron film between 6.4 nm to 9.9 nm thickness as estimated from preliminary XPS measurements. XPS data of freshly prepared iron films are generally showing only small oxygen contaminations well below 10 at.%. Sputtering of a freshly prepared iron film further reduces this contamination. Neither in MIES/UPS nor in XPS can any signal due to the W substrate be detected for an iron film of this thickness.

H_2O is offered via backfilling the chamber using a bakeable leak valve. The gas line is evacuated and can be heated in order to ensure cleanness. A quadrupole mass spectrometer (Balzers QMS 112A) is used to monitor the partial pressure of the reactive gases during experiments simultaneously to the MIES and UPS measurements. Water exposures of more than 10^3 L are offered in a preparation chamber attached to the UHV apparatus via a transfer system. It employs the same gas line as described above. For the experiments employing a water offer, the cleanness of deionised water is ensured by repeated pump-freeze-thaw cycles to remove any dissolved gases. Bake out of the gas lines and the careful cleaning of the water cannot exclude completely the presence of a small quantity of organic impurities.

3. Results

Fig. 1(a) shows MIES spectra obtained during the interaction of H_2O molecules with the Fe film. The spectra are displayed as a waterfall plot. The bottom spectrum shows a typical AN process for a clean iron surface [8]. With increasing H_2O offer, the peak beyond 12 eV binding energy, which is due to secondary electrons, increases and the shoulder around 5 eV, which is due to AN from Fe 3d states, vanishes. The spectra near saturation are still completely due to the AN process. The surface work function amounts to 4.2 eV. The details for the AN process will be discussed further in Section 4.

Fig. 1(b) shows the corresponding UPS spectra, which were recorded simultaneously with the MIES spectra. The bottom spectrum shows the clean iron film which is, besides the secondary electrons, dominated by the Fe 3d emission just below the Fermi level at a binding energy of 1 eV [8]. The Fe 3d signal decreases with increasing water offer, and a small contribution arises at 5.6 eV which is due to emission from O 2p orbitals [8]. Even for a water exposure of about 10^3 L a metallic contribution (meaning occupied states just below the Fermi level) remains visible.

To investigate a very high H_2O exposure, the sample is treated in the attached preparation chamber (see Section 2). A freshly prepared iron film is exposed to $2.7 \cdot 10^9$ L H_2O (1 mbar for 60 min). The sample is then transferred back into the UHV analysis chamber for measurement. The MIES and UPS results are shown in Fig. 2. MIES shows a peak doublet at 6 eV and 10.5 eV. These binding energies deviate by about 1 eV compared with those from the well-known OH molecular orbitals 1π and 3σ [25]. Also their peak height ratio and their relative energetic distance are not comparable to that of the OH doublet. A similar, but broader doublet structure is observed in UPS. These structures will be discussed in Section 4. Because MIES and UPS show the same doublet at the same energies, the corresponding electrons in MIES must be produced by the AD process, although the spectrum is still dominated by the AN process. The work function of this film is found to be 4.0 eV.

Fig. 3**(a)** shows the XPS spectrum from the iron Fe 2p range for the H_2O exposure of 840 L. For all following Fe evaluations, only Fe $2p_{3/2}$ is analyzed which was shown to give reliable results [8,26–29]. The Fe $2p_{1/2}$ is used as reference for the fitting procedure that bases on the works of Lin et. al., McIntyre et al. and Brundle et al. [26–28]. All binding energies and FWHMs evaluated in this paper are summarized in Table 1, constraints for the fitting procedure are typed in bold letters. In the figure, the original data is shown as dots. The calculated fit of this data is plotted in a line-style. In doing so, the green lines represent the sub-peaks and the red line shows the sum of all sub-peaks. Basing on our previous work for the interaction of oxygen with iron films [8] the fitting of the Fe $2p_{3/2}$ peak was performed in the following way:

1. The FWHM of Fe^0 is fixed to 2.27 eV. The FWHMs of the other three peaks are free for optimization by the fitting procedure. They must be expected to be in the range between 4.5 eV and 5.5 eV.
2. The relative energetic distance for $Fe^{2+} \Leftrightarrow Fe^{3+}$ is fixed at the value of 1.0 eV. The relative energetic distance for $Fe^0 \Leftrightarrow Fe^{2+}$ is expected to be in the range between 2.3 and 2.6 eV [8], but is not fixed during the fitting procedure.
3. The peak areas of Fe $2p_{3/2}$ and Fe $2p_{1/2}$ must amount to 2 : 1. This value is not fixed during the fitting procedure but is used as check for the fitting quality.
4. We allow for a fourth peak corresponding to a satellite (discussed below). Its position and FWHM are free during the fitting, and are used for a quality check of the fitting procedure.

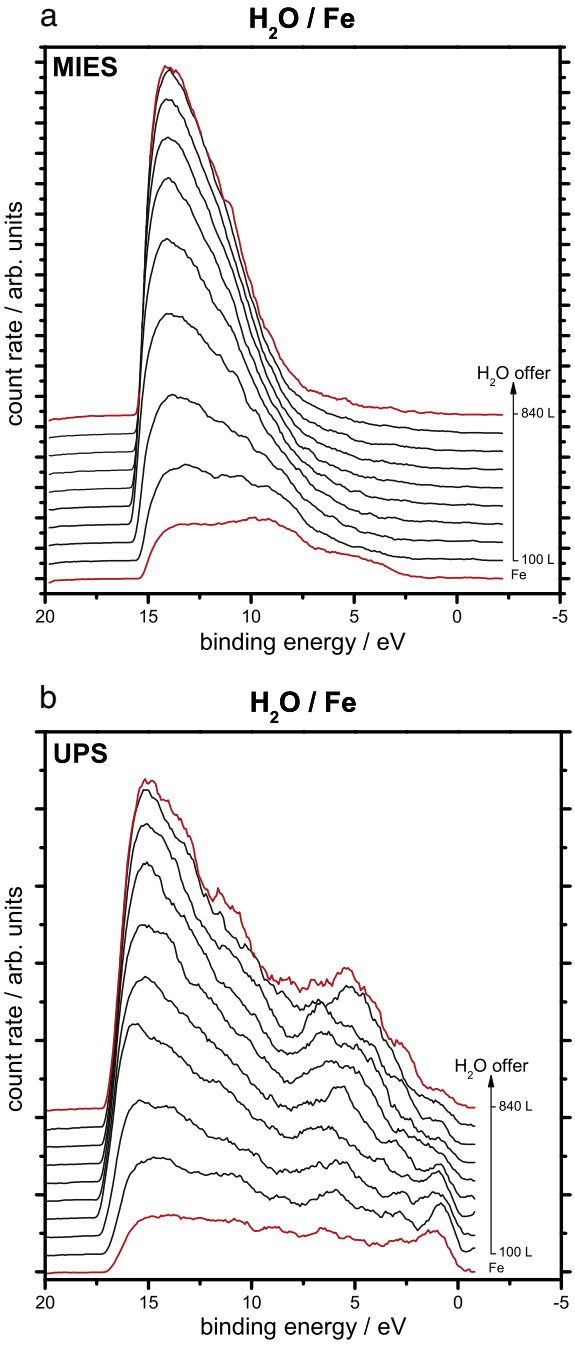

Fig. 1. MIES (a) and UPS (b) spectra during water offer to the iron film. The bottom spectrum shows the clean iron. The top spectrum corresponds to a final water offer of 840 L (corresponding to the XPS spectra in Fig. 3(a) and (b)).

In Fig. 3(a) the metallic contribution Fe^0 is found at the low binding energy side at 707.7 eV with a FWHM of 2.27 eV. Its binding energy differs up to 0.7 eV from literature [26–28] for all measurements. In Table 1 it can be seen that this is a constant offset which we find

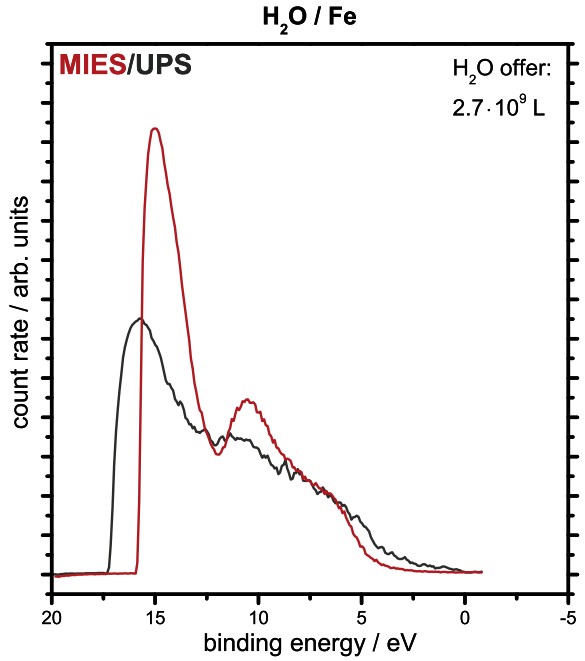

Fig. 2. MIES and UPS spectra for the iron film exposed to $2.7 \cdot 10^9$ L of water offer (corresponding to the XPS spectra in Fig. 4(a) and (b)). For preparation details see chapter 2.2.

for all peaks, because we did not scale our binding energies to any reference peak. Fe^{2+} is observed at 710.0 eV with a FWHM of 5.2 eV. The energetic distance between Fe^0 and Fe^{2+} amounts to 2.3 eV which corresponds well to literature [8,27,28]. Fe^{3+} is observed at 711.0 eV with a FHWM of 5.2 eV. Its energetic distance to the Fe^0 contribution amounts to 3.3 eV also corresponding well to literature [8,27,28]. At the high binding energy side between the Fe $2p_{3/2}$ and Fe $2p_{1/2}$ a well known peak is found (denoted by Fe^{sat}) at about 716.2 eV which is identified as Fe^{2+} satellite due to its energetic distance of 6.2 eV to the Fe^0 contribution [16,27,28,30].

Fig. 3(b) shows the XPS spectrum of the O 1 s range for a H_2O exposure of 840 L. The fitting of the O 1s peak was performed in the following way basing on [3,6,8]:

1. The FWHM of O 1s I is fixed to 2.0 eV. This is in accordance with our previous work [8] and with the literature [26]. The FWHM of the other contribution is free for optimization by the fitting procedure.
2. The relative energetic distance for O 1s I ⟺ O 1s II is fixed to 1.8 eV.

Two O 1s contributions are found at binding energies 530.7 eV (denoted by I) and 532.5 eV (denoted by II). The O 1s I contribution is assigned to the oxide formed at the surface. Their relative energetic distance adds up to 1.8 eV as described above. The FWHM of the O 1s II contribution amounts to 3.3 eV. As it is not possible to distinguish qualitatively and quantitatively between different oxidation states within the O 1s I contribution with XPS using our setup, no information on the amount of oxygen bound to Fe^{3+} or Fe^{2+} states can be drawn from these results. It cannot be excluded that different types of iron oxides are formed.

As was discussed previously with our experiments for the oxidation of iron films [8], we must emphasize that the O 1s II contribution at the high binding energy side of the O 1s peak does not account for adsorbed hydroxide groups although this was often announced in previous works, see for example [7,26,27]. The MIES and UPS spectra for the H_2O offer of about 10^3 L do not show any hydroxide contributions, although MIES is extremely sensitive for adsorbed OH groups [31]. The statement found quite frequently that O 1s II must be due

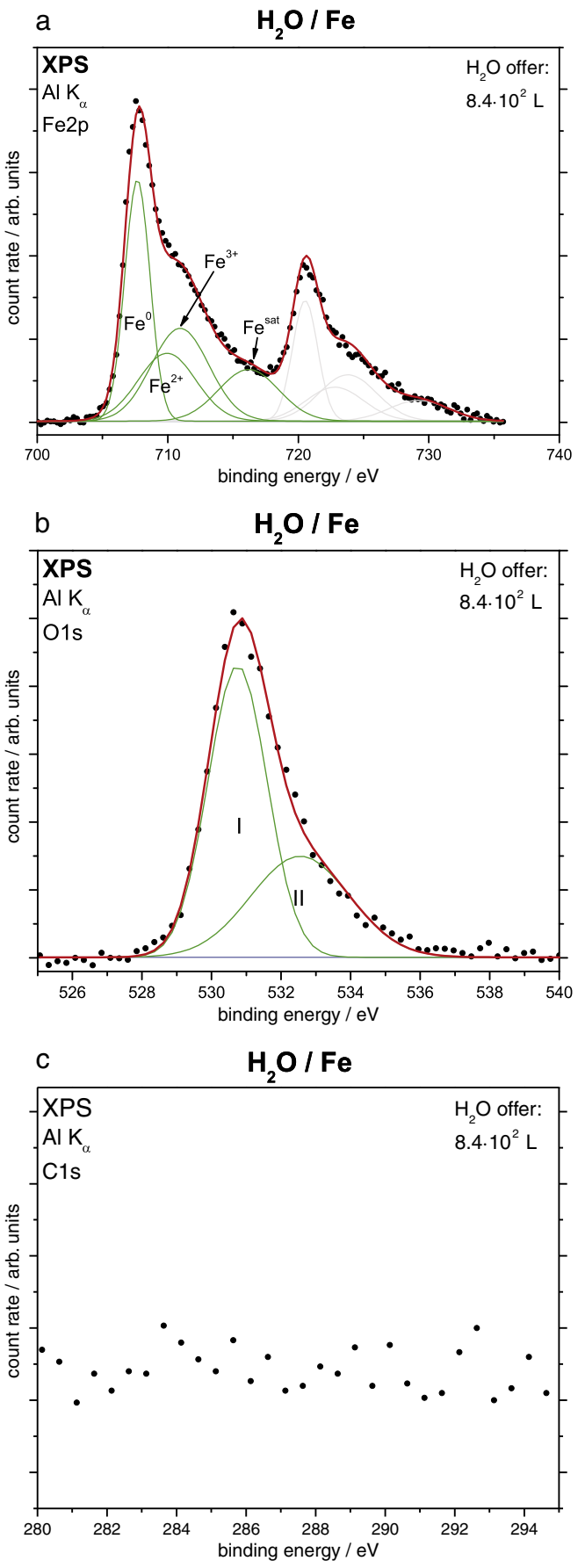

Fig. 3. XPS detail spectra from the iron film exposed to 840 L H_2O: (a) Fe 2p region, (b) O 1s region and (c) C 1s region (corresponding to Fig. 1 (a) and (b)).

Table 1
Summarized values of all XPS measurements (p denotes the valency; p = 2+, 3+).

System	Fig.	Peak	Fe 2p		O 1s		C 1s		Assignment	ΔE(Fe^p–Fe^0)	rel. intensity	d
			Energy	FWHM	Energy	FWHM	Energy	FWHM				
H_2O / Fe	3a	Fe^0	707.7	**2.27**					Fe^0			7.0 nm
($8.4 \cdot 10^2$ L)		Fe^{2+}	710.0	5.2					Fe^{2+}	2.3		Oxide:
		Fe^{3+}	711.0	5.2					Fe^{3+}	3.3		1.8 nm
	3b	I			530.7	**2.00**			Oxide		0.63	
		II			532.5	3.3			Adsorbate		0.37	
H_2O / Fe	4a	Fe^0	707.4	**2.27**					Fe^0			6.4 nm
($2.7 \cdot 10^9$ L)		Fe^{2+}	709.8	5.3					Fe^{2+}	2.4		Oxide:
		Fe^{3+}	710.8	5.3					Fe^{3+}	3.4		1.8 nm
	4b	I			530.4	**1.90**			Oxide		0.39	
		II			532.3	2.2			Adsorbate		0.39	
		III			533.4	4.1			C–O		0.22	
	4c	I					285.9	1.9	C–C, C–H		0.58	
		II					288.9	3.5	C–O, C=O		0.42	

to surface hydroxide formation is therefore disproved by our results. This is in agreement with Grosvenor [3], Gimzweski [6] and Brundle [28]. Basing on these works, the O 1s II contribution is assigned to excess oxygen that is chemisorbed at the surface but not incorporated into a well-ordered oxide.

Fig. 3**(c)** shows the XPS spectrum of the C 1s range for a H_2O exposure of 840 L. No signal is observed in this region. The ordinate uses the same scale as in Fig. 4(c). Hence, it can be excluded that any contamination with carbon and/or carbon compounds happens in the UHV chamber during the H_2O exposure.

Fig. 4**(a)** shows the XPS spectrum of the iron Fe 2p range after a H_2O exposure of $2.7 \cdot 10^9$ L. The treatment of the sample is described in detail in Section 2. The fitting of the Fe $2p_{3/2}$ peak was performed following the guideline described above with Fig. 3(a). The signal of the metallic contribution Fe^0 is found at the low binding energy side at 707.4 eV with a FWHM of 2.27 eV. Fe^{2+} is observed at 709.8 eV with a FWHM of 5.3 eV. Fe^{3+} is observed at 710.8 eV with a FHWM of 5.3 eV. All relative energetic distances between these peaks fit well to the literature and to the ones obtained for lower H_2O offers (see Table 1). Again we find the satellite peak, here at a binding energy of 716.5 eV. As already discussed above it is identified as the Fe^{2+} satellite.

Fig. 4**(b)** shows the corresponding XPS spectrum of the O 1s range for a H_2O exposure of $2.7 \cdot 10^9$ L. The fitting of the O 1s peak was performed in the following way:

1. The FWHM of O 1s I is fixed to 1.9 eV.
2. All other parameters were free for optimization by the fitting algorithms.

We find the three contributions at binding energies 530.4 eV (I), 532.3 ev (II) and 533.4 eV (III). The O 1s I contribution is again identified as oxide. Its energetic position is comparable to Fig. 3b. The relative energetic distance between the O 1s I and the O 1s II contribution has also a comparable value as evaluated in Fig. 3(b). The FWHM of the O 1s II contribution has a 1 eV smaller value as compared to Fig. 3(b). This is still supposed to be chemisorbed excess oxygen as described in Fig. 3(b). Due to the adsorption of another species (see Fig. 4(c)) a slighty changed chemical environment leads to the decrease of the FWHM. The relative energetic distance between the O 1s I and O 1s III contributions amounts to 3 eV. This chemical shift may indicate a bonding between carbon and oxygen atoms.

Fig. 4**(c)** shows the corresponding XPS spectrum of the C 1s range for H_2O exposure of $2.7 \cdot 10^9$ L. The scaling of the ordinate is the same as in Fig. 3(c). All parameters for the two proposed contributions were free during the fitting procedure. It is observed that the C 1s I contribution is located at a binding energy of 285.9 eV and the C 1s II contribution at a binding energy of 288.9 eV, accordingly. The FWHM for the C 1 s I contribution amounts to 1.9 eV. A value of 3.5 eV is obtained for the C 1 s II contribution. We therefore conclude that the contribution at the lower binding energy is assigned to elemental carbon or hydrocarbons adsorbed at the surface. Due to a chemical shift of 3 eV and a broad C 1 s II signal we suppose this contribution to originate from carboxyl and carbon oxide groups adsorbed to the surface. For the assignment of a carbon species to a specific C 1 s contribution see e. g. Gelius et al. [32].

4. Discussion

4.1. Water exposure of 840 L

The MIES spectra in Fig. 1(a) are completely governed by the Auger Neutralization process. For the pure Fe film (bottom spectrum) this behavior is well known. It is based on the fact that the 2s orbital of the impinging He^* $^3S_1$ atom is located above the surface Fermi level for a work function of 4.2 eV [19,20]. Therefore the 2s electron is resonantly transferred into unoccupied Fe surface states. Hence, the MIES spectra reflect the AN process. The broad peak around 4–5 eV is caused by a self-convolution of Fe 3d states located just below the Fermi level. With increasing H_2O exposure this contribution vanishes indicating the loss of occupied states below the Fermi level and the loss of the metallic character of the surface. Nevertheless, even at 840 L of water exposure the spectrum is still an AN spectrum. A similar behavior was also found for the interaction of O_2 with iron films [8]. The large work function of the grown iron oxide layer allows the resonant transfer of an electron from the He 2s level into unoccupied states of the surface and thus the deexcitation of the He^* via the AN process. From the comparison of MIES and UPS in Fig. 1 we find that UPS still shows a distinct amount of occupied Fe 3d just below the Fermi level. This means that the thickness of the oxide surface layer is only small.

Surprisingly, we do not find any traces of surface hydroxide groups which would show a peak doublet at 5.8 eV and 10.5 eV due to the ionization of the OH molecular orbitals 1π and 3σ [25]. MIES is a very surface sensitive technique, featuring an information depth of zero. This means that OH groups located on top of a surface would be visible very well. Furthermore, such molecules would hinder or at least reduce the resonant He 2s electron transfer. That would strongly reduce the probability for the AN process and strengthen the AD process. This is not observed though. We must therefore conclude that on top of the surface no hydroxide is formed at all. UPS (Fig. 1(a)) shows a peak at a binding energy of around 5.5 eV corresponding to O 2p emission and XPS (Fig. 3(b)) very clearly shows the existence of an O 1s signal. We conclude that for H_2O exposures up to 840 L impinging H_2O molecules are dissociated completely. The remaining oxygen atoms are incorporated into the

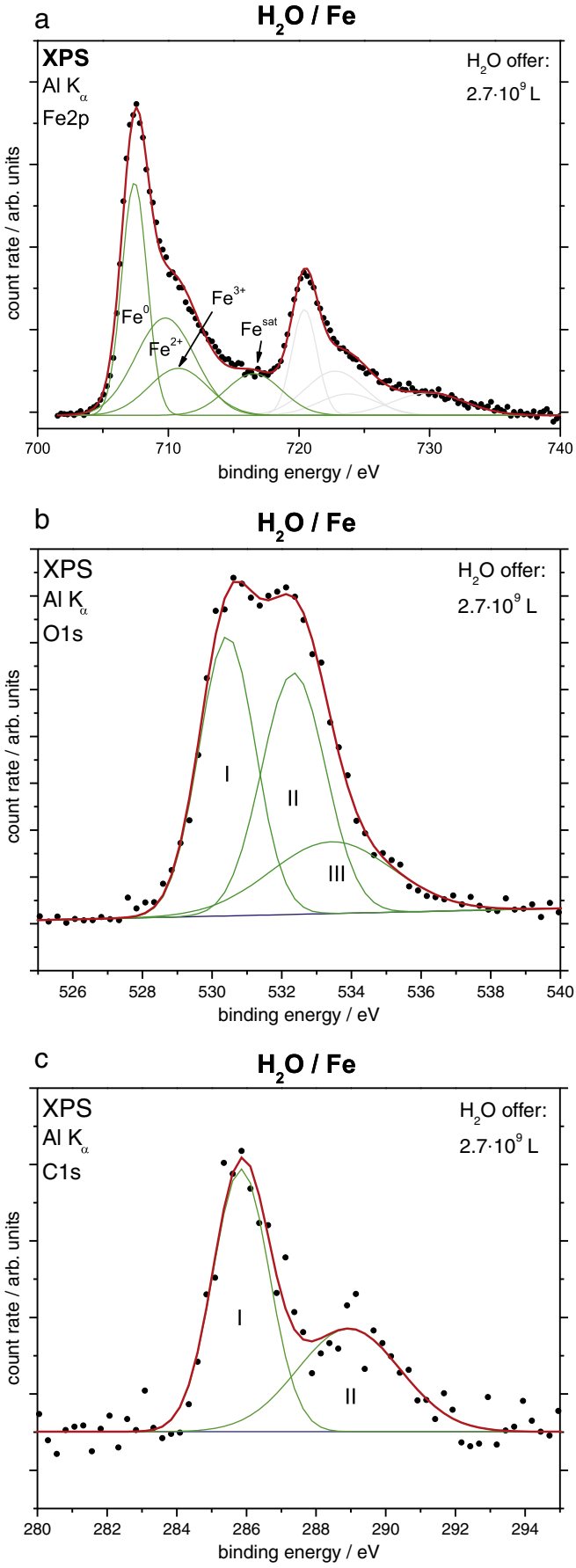

Fig. 4. XPS detail spectra from the iron film exposed to $2.7 \cdot 10^9$ L H_2O: (a) Fe 2p region, (b) O 1s region and (c) C 1s region (corresponding to Fig. 2).

iron film while the H atoms are desorbed, most likely after recombination to H_2. Similar dissociation processes were previously observed for example on Sr [25] and Ca [31].

At an exposure of around 840 L MIES and UPS spectra appear to be saturated, no further changes occur even for increased water exposures under UHV conditions. Obviously, the surface oxide layer hinders the further dissociation of impinging H_2O molecules.

Beside the main O 1s I peak, XPS shows a second contribution at 1.8 eV higher binding energies. Again, this peak does not correspond to any hydroxide feature which is proven by the absence of any hydroxide features in MIES. As already discussed previously for the interaction of oxygen molecules with iron and for Fe_2O_3 powder samples, we interpret this peak as oxygen atoms which are not well incorporated into the surface oxide layer, but just being chemisorbed on the surface [8,28].

On the basis of the Fe^0 (denoted as I_m), Fe^{2+} and Fe^{3+} XPS peak intensities we are able to calculate the oxide layer thickness d [33]:

$$d = \lambda_o \cos\Theta \ln\left[\left(\frac{D_m\lambda_m}{D_o\lambda_o}\right)\left(\frac{I_o}{I_m}\right)+1\right] \quad (2)$$

The integral intensities of the Fe^{2+} and Fe^{3+} are denoted as I_o. λ_m is the inelastic mean free path (IMFP) of photoelectrons originating from the Fe^0 contribution. λ_o depicts the IMFP of photoelectrons having their origin in the oxide. As a first approximation, it has been calculated using [18] on the assumption of a FeO formation in the surface layer. However this is only an approximation because there may be several different types of iron oxides formed at the surface. D_m and D_o denote the atomic number densities in the metal and in the oxide, respectively.

Applying this we find an oxide layer thickness for the Fe film exposed to 840 L of H_2O of 1.8 nm. A similar value for the oxide layer thickness is found in [7]. It appears to be very likely keeping in mind the observation that UPS still shows a metallic character of the surface by occupied Fe 3d orbitals, although the information depth of UPS is very small.

4.2. Water exposure of $2.7 \cdot 10^9$ L

The MIES spectrum in Fig. 2 is governed by the two distinct peaks at 6 eV and 10.5 eV. These peaks are proposed to originate from carboxyl and hydrocarbon groups adsorbed at the surface. The reader has been referred to the fact before that the sample is treated in the preparation chamber. Therein the water partial pressure amounts to 1 mbar which is held for 60 min. This high partial pressure is chosen regarding to the fact that the aspect of corrosion is studied for a thick iron layer. Nevertheless, this high partial pressure and the long exposure time leads unavoidably to impurities within the gas atmosphere resulting in the adsorption of contaminants on the surface. The reader may take into account that the carefully cleaned water reservoir (as described in the experimental section) is at last containing some organic impurities. These impurities may amount to approximately 1 ppm. Then it can be easily calculated that at a H_2O partial pressure of 1 mbar and an exposure time of 3600 s about 2700 L of carbon containing compounds are offered to the surface.

As the AN process dominates, the single observation of adsorbed carboxyl and hydrocarbon group is still surprising. Compared to other systems, e. g. Ca or Al, the offer of H_2O to these surfaces leads to a fast oxidation and adsorption of hydroxide groups within a few Langmuir. In this case, even after a high exposure beyond 10^9 L, the initial iron oxide layer inhibits further surface reactions. The AN process still dominates and no OH groups are identifiable in the spectrum.

In UPS just below the Fermi level, there are still contributions due to occupied Fe 3d orbitals visible. This is accompanied by the observation of a Fe^0 contribution in XPS. Furthermore, the oxide layer

thickness does not change compared with the lower dose of 840 L. Applying Eq. (2), we calculate the oxide layer thickness for the exposure of $2.7 \cdot 10^9$ L to 1.8 nm. This means that even for an exposure of more than 10^9 L of H_2O the oxide layer thickness does not grow.

According to the lower dose, the XPS O 1s signal recorded after the exposure of $2.7 \cdot 10^9$ L H_2O can be fitted with two Gaussian peaks. If compared to Fig. 3(b), the FWHM of O 1s II in Fig. 4(b) as the only free fitting parameter is almost equal to the value observed before. Only the relative intensities (according to the complete O 1s signal) of both contributions change due to the high H_2O dose. The ratio of 0.74 for the O 1s II is twice as large as for the exposure of 840 L. This means a higher fraction of the adsorbed oxygen is now assigned to adventitious oxygen.

Furthermore, the XPS C 1s signal observed after the exposure of $2.7 \cdot 10^9$ L H_2O shows the difficulty to obtain a clean water atmosphere at this high water partial pressure of 1 mbar. The adsorbed carbon species may result from organic impurities dissolved in the water which can be estimated to have portion of less than 1 ppm. Even with this estimate, one can quickly see that for the chosen partial pressure and exposure time, a significant contamination is not avoidable.

Taking into account the constant oxide layer thickness of 1.8 nm for a wide exposure range we propose a model for the interaction of H_2O molecules with iron films close to the model for the O_2 interaction with Fe films [8]. In the first step, the complete dissociation of the H_2O molecules leads to the oxidation of the iron layer. After the formation of a complete and closed oxide surface layer, the sticking coefficient for oxygen is zero [34]. Further impinging water molecules cannot be dissociated completely any longer on top of this passivating oxide layer. This means that no oxygen atoms are produced in the vicinity of the surface. The dissociation is inhibited by the lack of charge density near the Fermi level. Obviously, a very small probability for partly dissociation remains.

These results contradict the previous picture proposed by Roberts and Wood [7]. They suggest a $FeO \cdot OH$ layer with a maximum thickness of about 5 Å. Such an overlayer should be certainly detected by UPS and MIES. In a second aspect, they varied H_2O partial pressures and exposure times. A high H_2O partial pressure and a short exposition time reduces the danger of impurity adsorption, but it also cannot be completely excluded for example for the case of $1 \cdot 10^{-1}$ mbar and 30 min exposure. For this kind of experiments, the XPS data of the C 1s region have to be shown necessarily. We challenge the picture of such an overlayer as we found no evidence in UPS and MIES. Certainly and in agreement with [7], a stable and passivating oxide layer is formed as an iron surface is solely exposed to water. From the aspect of corrosion, this is a surprising result.

Rust formation is a three step process as illustrated in the introduction. The formation of a thin oxide layer of with a thickness of 1.8 nm during low H_2O exposures is in accordance with step 1 of this process. Nevertheless, this oxide layer is stable and remains unchanged even for very high H_2O partial pressures of 1 mbar. This contradicts the common knowledge of the instability of iron towards aqueous environments. Obviously, only the impact of additional atmospheric components like reactive gases, liquid water, aerosols and/or UV irradiation leads to the rust formation as pointed out in step 2 [1,2]. Our results for the interaction of water with iron reveal the passivation behavior of iron for aqueous environments under the applied conditions.

5. Summary

The interaction of water at exposures of 10^3 L to more than 10^9 L to iron films was studied by XPS, MIES and UPS.

UPS measurements of the clean iron films show a metallic behavior dominated by the Fe 3 d contributions just below the Fermi level. These contributions decrease during water exposure while the O 2p emission increases accordingly. This indicates the formation of iron oxide surface layers. No OH 1π and 3σ emission is observed at a water offer of 840 L. As the water offer is increased to $2.7 \cdot 10^9$ L, only a less intense and broad contribution resulting from the adsorption of hydrocarbons become visible corresponding to the adsorption of impurities.

MIES of the clean iron film is completely dominated by the well known Auger Neutralization process. The interaction process does not change due to the ongoing formation of the iron oxide film during the water exposure of 840 L. This behavior was also found during the interaction of oxygen molecules with iron surfaces. Only at the very high water exposures beyond 10^9 L we observe Auger Deexcitation from carboxyl and hydrocarbon impurities adsorbed at the surface. Thus, both UPS and MIES do not show the formation of an overlayer by adsorbed OH groups.

In XPS, a significant signal contribution belonging to metallic iron is still found even for saturation water offer. We find an oxide layer with a thickness of 1.8 nm for low water exposure as well as for the very high water exposure.

The combination of MIES, UPS and XPS for water saturated iron films shows that carbon impurities are adsorbed for very high water exposures of $2.7 \cdot 10^9$ L. The formed iron oxide film is very stable, even in the case of coadsorption of other species.

This behaviour is attributed to a passivating effect of the surface oxide layer that inhibits dissociation of impinging molecules due to missing electron density directly below the Fermi level. Obviously, this characteristics of the iron surface is different to observations under ambient conditions.

Acknowledgements

We thankfully acknowledge technical assistance by Denise Rehwagen.

References

[1] C. Leygraf, T.E. Graedel, Atmospheric Corrosion, Wiley Interscience, New York, 2000.
[2] H. Kaesche, Corrosion of Metals, Springer Verlag, Berlin, 2003.
[3] A.P. Grosvenor, B.A. Kobe, N.S. McIntyre, Surf. Sci. 572 (2004) 217.
[4] S.J. Roosendaal, J.P.R. Bakker, A.M. Vredenberg, F.H.P.M. Habraken, Surf. Sci. 494 (2001) 197.
[5] B.L. Maschhoff, N.R. Armstrong, Langmuir 7 (1991) 693.
[6] J.K. Gimzewski, B.D. Padalla, S. Affrossman, L.M. Watson, D.J. Fabian, Surf. Sci. 62 (1977) 386.
[7] M.W. Roberts, P.R. Woods, Electron. Spectrosc. Relat. Phenom. 11 (1977) 431.
[8] K. Volgmann, F. Voigts, W. Maus-Friedrichs, Surf. Sci. 604 (2010) 906.
[9] Y. Yamauchi, M. Kurahashi, Appl. Surf. Sci. 169–170 (2001) 236.
[10] Y. Yamauchi, M. Kurahashi, T. Suzuki, Jpn. J. Appl. Phys. 41 (2002) 4675.
[11] T. Suzuki, M. Kurahashi, Y. Yamauchi, Surf. Sci. 476 (2001) 63.
[12] S. Förster, G. Baum, M. Müller, H. Steidl, Phys. Rev. B 66 (2002) 134427.
[13] S. Tougaard, Surf. Sci. 216 (1989) 343.
[14] D.A. Shirley, Phys. Rev. B 5 (1972) 4709.
[15] T. Yamashita, P. Hayes, Electron. Spectrosc. Relat. Phenom. 152 (2006) 6.
[16] E.J. Paparazzo, Electron. Spectrosc. Relat. Phenom. 154 (2006) 38.
[17] J.H. Scofield, J. Electron. Spectrosc. Relat. Phenom. 8 (1976) 129.
[18] National Institute of Standards and Technology Electron Inelastic-Mean-Free-Path Database 1.1, http://www.nist.gov/srd/nist71.htm.
[19] Y. Harada, S. Masuda, H. Ozaki, Chem. Rev. 97 (1997) 1897.
[20] H. Morgner, Adv. At. Mol. Opt. Phys. 42 (2000) 387.
[21] G. Ertl, J. Küppers, Low Energy Electrons and Surface Chemistry, VCH Verlag, Weinheim, 1985.
[22] M. Frerichs, F.X. Schweiger, F. Voigts, S. Rudenkiy, W. Maus-Friedrichs, V. Kempter, Surf. Interface Anal. 37 (2005) 633.
[23] M. Frerichs, F. Voigts, S. Hollunder, R. Masendorf, Appl. Surf. Sci. 252 (2005) 108.
[24] H. Bethge, D. Heuer, Ch. Jensen, K. Reshoft, U. Kohler, Surf. Sci. 331–333 (1995) 878.
[25] W. Maus-Friedrichs, A. Gunhold, M. Frerichs, V. Kempter, Surf. Sci. 488 (2001) 239.
[26] T.-C. Lin, G. Seshadri, J.A. Kelber, Appl. Surf. Sci. 119 (1997) 83.
[27] N.S. McIntyre, D.G. Zetaruk, Anal. Chem. 49 (1977) 1521.
[28] C.R. Brundle, T.J. Chang, K. Wandelt, Surf. Sci. 68 (1977) 459.
[29] T. Yamashita, P. Hayes, Appl. Surf. Sci. 254 (2008) 2441.
[30] T.A. Carlson, Discuss. Faraday Soc. 60 (1975) 30.
[31] F. Bebensee, F. Voigts, W. Maus-Friedrichs, Surf. Sci. 602 (2008) 1622.
[32] U. Gelius, et al., Phys. Scr. 2 (1970) 70.
[33] E. McCafferty, J.P. Wightman, Surf. Interface Anal. 26 (1998) 549.
[34] T.-U. Nahm, R. Gomer, Surf. Sci. 373 (1997) 237.